Research Article

Rapid Communications in Mass Spectrometry

Received: 4 December 2012 Revised: 18 January 2013 Accepted: 18 January 2013 Published online in Wiley Online Library

Rapid Commun. Mass Spectrom. **2013**, *27*, 816–824
Published online Wiley Online Library (wileyonlinelibrary.com) DOI: 10.1002/rcm.6519

Electronic structure and gas-phase chemistry of protonated α- and β-quinonoid compounds: a mass spectrometry and computational study

Ricardo Vessecchi[1]*, Flávio S. Emery[2], Norberto P. Lopes[1] and Sérgio E. Galembeck[3]

[1]Núcleo de Pesquisa em Produtos Naturais e Sintéticos, Departamento de Física e Química, Faculdade de Ciências Farmacêuticas de Ribeirão Preto, Universidade de São Paulo, Brasil
[2]Departamento de Ciências Farmacêuticas, Faculdade de Ciências Farmacêuticas de Ribeirão Preto, Universidade de São Paulo, Brasil
[3]Departamento de Química, Faculdade de Filosofia, Ciências e Letras de Ribeirão Preto, Universidade de São Paulo, Brasil

RATIONALE: The use of quinonoid compounds against tropical diseases and as antitumor agents has prompted the search for new naturally occurring and synthetic derivatives. Among these quinonoid compounds, lapachol and its isomers (α- and β-lapachone) serve as models for the synthesis of new compounds with biological activity, and the use of electrospray ionization tandem mass spectrometry (ESI-MS/MS) analysis as a tool to elucidate and characterize these products has furnished important information about these compounds.
METHODS: ESI-MS/MS analysis under collision-induced dissociation conditions was used to describe the fragmentation mechanisms for protonated 1,4-naphthoquinone, 1,2-naphthoquinone, α-lapachone, and β-lapachone. The B3LYP/6-31+G(d,p) model was used to obtain proton affinities, gas-phase basicities, and molecular electrostatic potential maps, thus indicating the probable protonation sites. Fragmentation pathways were suggested on the basis of the relative enthalpies of the product ions.
RESULTS: The ESI-MS signals of the cationized molecules of *ortho* quinonoid compounds were more intense than those of the protonated molecule. Formation of the major product ions with *m/z* 187 from protonated α- and β-lapachone has been attributed to a retro-Diels-Alder (RDA) reaction.
CONCLUSIONS: MS/MS studies on lapachol isomers (α- and β-lapachone) will facilitate the interpretation of the liquid chromatography (LC)-MS/MS analysis of new metabolites. MS/MS data on the 1,4-naphthoquinone, 1,2-naphthoquinone, α-lapachone and β-lapachone core will help characterize new derivatives from *in vitro*/*in vivo* metabolism studies in complex matrices. The product ions revealed the major fragmentation mechanisms and these ions will serve as diagnostic ions to identify each studied compound. Copyright © 2013 John Wiley & Sons, Ltd.

The use of quinonoid compounds against tropical diseases[1,2] and as antitumor agents[3] has prompted the search for new naturally occuring[4] and synthetic derivatives.[5,6] As a result, several research groups have focused on the synthesis of new *ortho*- or *para*-quinonoid compounds,[5–7] to gain knowledge about their reactivity and activity as antitumoral,[8] molluscicidal,[9] leishmanicidal,[10] and anti-inflammatory[11] agents. Among quinonoid compounds, lapachol[12] and its isomers (α- and β-lapachone)[13] can serve as model for the synthesis of new compounds with biological activity. Electrochemical methods have been used to characterize these compounds,[14] furnishing insight into how these new compounds act.[14]

* *Correspondence to:* R. Vessecchi, Núcleo de Pesquisa em Produtos Naturais e Sintéticos (NPPNS), Departamento de Física e Química, Faculdade de Ciências Farmacêuticas de Ribeirão Preto, Universidade de São Paulo, Via do Café, S/N – CEP, 14040-903,Ribeirão Preto/SP, Brasil.
E-mail: vessecchi@bol.com.br; vessecchi@usp.br

The advent of mass spectrometry (MS) with modern ionization sources, such as electrospray ionization (ESI)[15] and matrix-assisted laser desorption/ionization (MALDI),[16] has contributed to the analysis of thermolabile molecules.[15,16] Sequential MS analysis (MS/MS)[17,18] is the main tool to elucidate and characterize natural products, and new derivatives from *in vitro* biotransformation.[18–20] In addition, previous knowledge of the fragmentation pathways of a series of compounds exhibiting a conserved structural core is useful for structural elucidation based on spectral libraries.[17–20] As a result, information about these compounds can be used in metabolomic studies.[18,20]

ESI in combination with MS/MS analysis can be used to elucidate the gas-phase chemistry of several classes of natural compounds.[21,22] The number of studies on quinones has increased,[21–24] because these compounds have interesting electrochemical behavior in the ESI source.[25] The protonated and deprotonated species of 1,4-naphthoquinone can occur during ESI analysis,[21,22] and the radical anion has also been detected.[25] Several papers have described the gas-phase reactivity of quinonoid compounds by combining ESI studies

Rapid Communications in Mass Spectrometry

with computational chemistry.[21–25] However, dissociation of the protonated 1,4-naphthoquinone (**1**) and 1,2-naphthoquinone (**2**) has not been investigated (Fig. 1). Comparison of the properties (reactivity, protonation, and dissociation) of *ortho*-naphthoquinone and *para*-naphthoquinone provides information about how conjugation affects these systems and more complex quinonoid moieties.[26]

We have previously reported on the versatile reactivity of lapachol and its congeners (2-hydroxy-1,4-naphthoquinone derivatives) under ESI and CID conditions.[24] The major fragmentation channels were assessed and used in further studies on its derivatives. The MS/MS investigation of lapachol isomers, such as α- and β-lapachone (Fig. 1, structures (**3**) and (**4**)) should help create a spectral data bank, to understand the fragmentation and reactivity of new derivatives of these compounds. In addition, the use of mass spectrometry for the elucidation of *in vitro* and *in vivo* metabolites from lapachol has been demonstrated, and α- and β-lapachone were the major secondary metabolites observed in these studies.[27,28] To date, only electron ionization (EI-MS) results are available for compounds (**1**)–(**4**).[29,30] The EI-MS structural determination of (**1**) and (**2**) has been reported.[30] Compound $(\mathbf{1})^{+\cdot}$ undergoes consecutive CO eliminations. The major EI fragments ions occur at *m/z* 130 and 102, and the main difference between $(\mathbf{1})^{+\cdot}$ and $(\mathbf{2})^{+\cdot}$ is the relative intensity of these ions. Recent studies on the metabolism of (**4**) by ESI-MS/MS and high-resolution analysis have helped describe its metabolites *in vitro*.[20,27,28] However, the authors did not elucidate the dissociation mechanisms, and there is a need for more advanced analysis.

In this work, we describe the fragmentation mechanisms for protonated 1,4-naphthoquinone (**1**), 1,2-naphthoquinone (**2**), α-lapachone (**3**), and β-lapachone (**4**) under collision-induced dissociation (CID). The reactivity sites were determined through computational quantum chemical models.[31] The stability of each product ion was described on the basis of the relative enthalpies and Gibbs energies calculations that revealed the major fragmentation mechanisms.

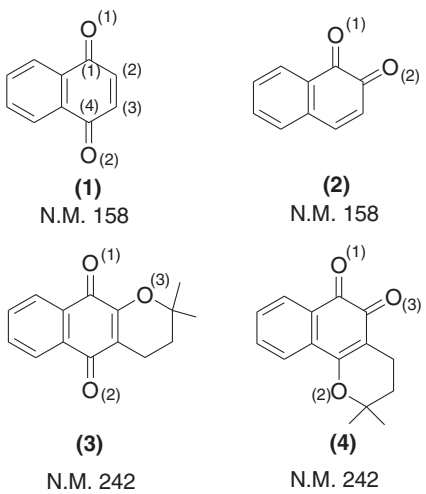

Figure 1. Structure of naphthoquinones: (**1**) 1,4-naphthoquinone; (**2**) 1,2-naphthoquinone; (**3**) α-lapachone; (**4**) β-lapachone. N.M. are the nominal masses in *u*. (Atom labels for 1,4- and 1,2-naphthoquinone are shown in Supplementary Fig. S1, see Supporting Information.)

MS/MS data on the α-lapachone or β-lapachone core will help characterize new derivatives from *in vitro*/*in vivo* metabolism studies.[20,27,28]

EXPERIMENTAL

Synthesis

1,4-naphthoquinone (**1**) and 1,2-naphthoquinone (**2**) were purchased from Sigma-Aldrich Brazil Ltda (Sao Paulo, Brazil). Lapachol was obtained from *Tabebuia avellanedae* Lor. ex Griseb, as described by Paternò.[32] Lapachol cyclization to α- and β-lapachone [(**3**) and (**4**)] was achieved following the methodology of Hooker,[33] which gave the α-isomer by reflux of lapachol with hydrochloric acid/acetic acid (1:4) at ambient temperature. To obtain the β-isomer, lapachol was dissolved in sulfuric acid (Scheme 1). The structures were confirmed by spectroscopic analysis.

Mass spectrometry analysis

The stock solutions of (**1**), (**2**), (**3**), and (**4**) for MS analysis were prepared from a 0.05 $mg.mL^{-1}$ solution of each compound in acetonitrile/water (9:1 v/v).

The high-resolution (HR) ESI-MS analyses were carried out on a hybrid quadrupole (Q)/time-of-flight (TOF) mass spectrometer (UltroTOF-Q, Bruker Daltonics, Billerica, MA, USA) fitted with an ESI source that was operated in positive mode. Samples were directly infused into the ionization source at a flow rate of 10 $\mu L.min^{-1}$. The source block and desolvation temperature was 150 °C. The accurate masses were obtained by using sodium trifluoroacetate as the mass standard, after each analysis, and the proposed formulae for each ion (protonated and cationized molecules) were based on errors being less than 5 ppm from the calculated mass. The voltage applied at the capillary emitter was optimized (2.5 kV), in order to achieve a high relative intensity of protonated $[M+H]^+$ or cationized molecules ($[M+Na]^+$ or $[M+K]^+$).

For the MS/MS analysis, the precursor ion (protonated molecule) was selected with an isolation width of 0.5 *m/z* units and fragmented by CID, using N_2 as the collision gas. Initial CID spectra in low resolution of the precursor ions were obtained at E_{lab} of 5, 10, 15, 20, 25, 30, 35, and 40 eV. Energy-resolved plots[34] were constructed from the relative intensity of the precursor and product ions, for better understanding of the dissociation processes undergone by the protonated molecules.

Computational methods

All the molecules had their geometries optimized by the B3LYP/6-31+G(d,p) model,[35,36] using the Gaussian 03 suite of programs.[37] Geometry analysis for 1,4-naphthoquinone[25] and 2-hydroxy-1,4-naphthoquinone[38] obtained

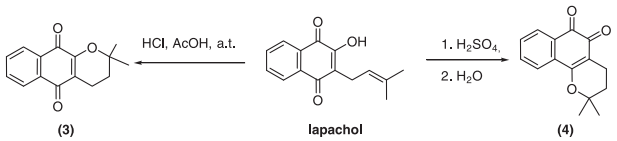

Scheme 1. Preparation of lapachol derivatives.

by the B3LYP/6-31+G(d,p) model (Supplementary Table S1, Supporting Information) showed that the bond lengths agreed with those from the X-ray diffraction experiments.[39] The B3LYP model also furnished the most exact thermochemical parameters for the quinonoid compound derivatives.[40] Protonation sites were proposed on the basis of the atomic charges described by the Merz-Singh-Kollman (MK) scheme,[41] the molecular electrostatic potential map (MEP) generated from the electronic density, HOMO analysis, gas-phase basicities (GBs), and proton affinities (PAs).[31] The MEP is the potential energy of interaction of a proton with the charge distribution generated by the nuclei and electrons of a molecule. The GBs and PAs were obtained by variations of Gibbs energies and enthalpies for a protonation reaction $M+H^+ \rightarrow MH^+$, respectively.[31]

The quantum theory of *atoms-in-molecules* (AIM)[42] was applied, so as to gain insight into the changes in bond strength after protonation.[40,43] The molecular graphs (a representation of the structure of a chemical compound, whose vertices correspond to the atoms of the compound and edges correspond to chemical bonds)[42] were plotted with the aid of the AIM 2000 software.[44]

The fragmentation pathways were suggested by calculation of the Gibbs energies and enthalpies at 298.15 K, and the product ions were proposed. The corresponding transition state (TS) energies were obtained and reported relative to that of the respective precursor (named as critical energy), which was characterized by one imaginary vibrational frequency. Molekel 4.3[45] was employed for visualization of some of the examined properties.

RESULTS

Protonation sites and electronic structure

To purpose the fragmentation mechanism, we searched for the most favorable site for proton attachment. Quantum descriptors were used to describe the protonation site in our early studies, and the results agreed with thermochemical calculation data.[21,22,31,40] For (**1**) and (**2**), atomic charge analysis (Supplementary Table S2, Supporting Information) in combination with HOMO and MEP (Figs. 2 and 3) confirmed that the oxygens are the most nucleophilic atoms in the molecules. For (**3**) and (**4**), the most nucleophilic sites were the same oxygen atoms and C(3), as depicted in Fig. 3. As previous studies with naphthoquinones had shown that protonation on C(3) was less favorable (lower values of PA and GB) than that on O(1), O(2) and O(3),[46] PAs and GBs were determined for oxygen protonation only. It has been shown that PA and

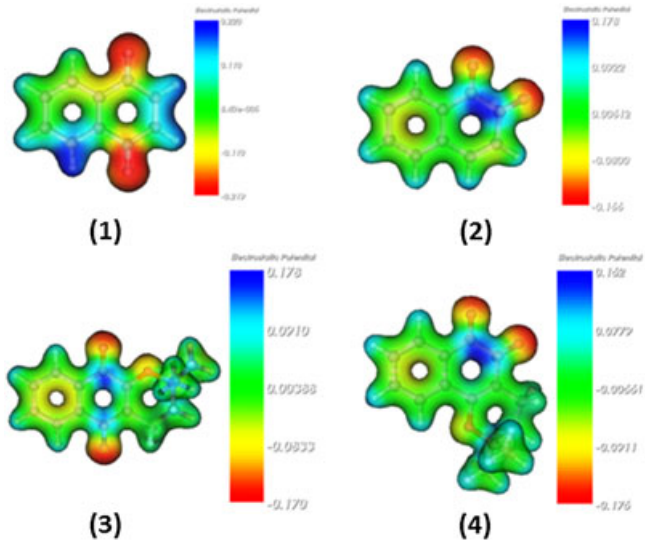

Figure 2. Molecular electrostatic potential map (MEP) for quinonoid compounds (**1**)–(**4**) plotted at the surface of electron density equal to 0.05 e/Bohr^3. Red regions are attractor to positive charge; as instance, a proton.

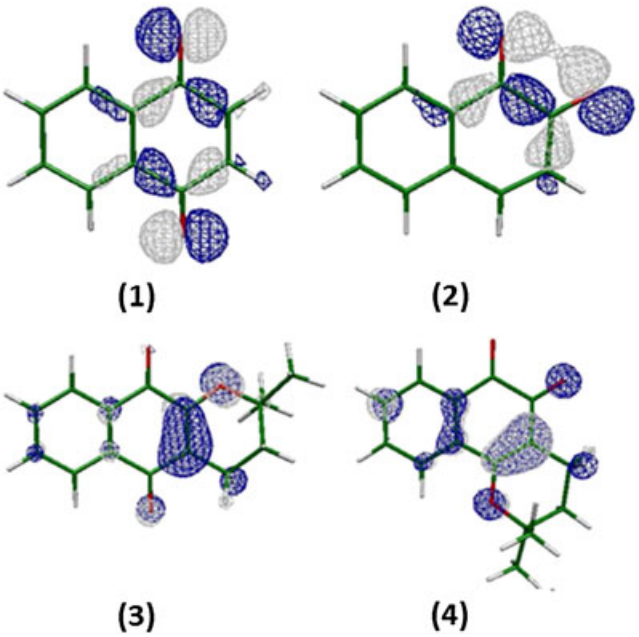

Figure 3. HOMO (highest occupied molecular orbital) for the quinonoid compounds.

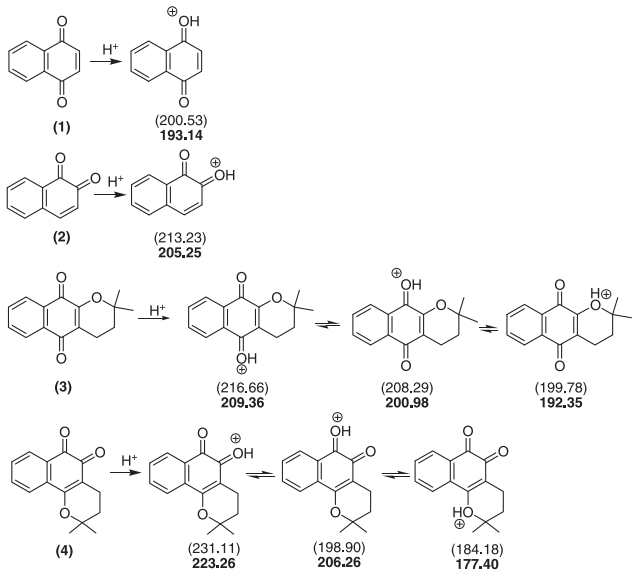

Scheme 2. Proton affinities (in parentheses) and gas-phase basicities (bold) for the protonated molecules. All the values are in kcal mol^{-1}.

Rapid Communications in Mass Spectrometry

GB values are important descriptors to interpret protonation in ESI-MS.[25,46,47]

According to PA and GB analysis the most reactive site for all the compounds is the quinonoid carbonyl (Scheme 2). The basicity of (**1**) is higher than that of (**2**), suggesting that protonation occurs between the two oxygen atoms, which can be stabilized through an intramolecular hydrogen bond (HB) (Fig. 4). AIM analysis and geometry parameters indicated formation of an intramolecular HB after protonation (Fig. 4). The ρ and $\nabla^2\rho$ values for a possible intramolecular HB agree with those described by Koch and Popelier.[48]

The PA and GB values indicate that the protonation site for (**3**) is the O(2) atom (Scheme 2), which can be explained by the mesomeric effect from the lone pair of O(3), as was shown in studies on 2-hydroxy-1,4-naphthoquinone derivatives.[46] These results agree with those from the MEP analysis, where O(2) was indicated as the most nucleophilic site. For (**4**), the PA and GB values suggest that protonation again takes place at the O(3) atom, where a possible HB stabilizes the protonated molecule, as depicted in Fig. 4 for (**2**). Resonance in the quinonoid system can also contribute to stabilize this protonation site. The same explanation applies for the higher value of PA and GB of (**4**) than of (**3**).

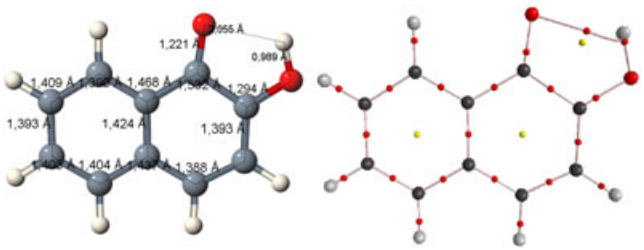

Figure 4. Geometry for the equilibrium structure (left) and molecular graph (right) of $[(\mathbf{2})+H]^+$. The occurrence of BCP (bond critical point) and BP (bond path) between O(2)-H--O(1), 2.055 Å, indicates the presence of HB. For more details, see Bader[42] and Koch and Popelier.[48]

Mass spectrometry studies and fragmentation mechanisms

The ESI-MS spectra of (**1**) and (**2**) reveal several differences (Fig. 5). For (**1**) the base peak in the ESI-MS spectrum is the $[(\mathbf{1})+H]^+$ ion at *m/z* 159.0441 (Table 1). For (**2**), the base peak is the $[(\mathbf{2})+Na]^+$ ion at *m/z* 181.0272. The same observations apply for the spectra of (**3**) and (**4**) (Fig. 5). The easy occurrence of $[M+Na]^+$ ions for (**2**) and (**4**) is due to the presence of vicinal carbonyls at the quinonoid moiety, which stabilize the sodiated molecules, through electrostatic interaction with the lone pairs of the oxygen atoms. Thus, the β-quinonoid system can act as sequestering agents, interacting with the cation.

The sodiated dimer of (**4**) at *m/z* 507.1768 is more intense than that of (**3**) at *m/z* 507.1767 (Fig. 5 and Table 1), and this can be attributed to the lone pairs of electrons on the vicinal carbonyls, as observed in studies with lapachol.[24] The same behaviour was observed for the $[2M+K]^+$ ions.

The relative ESI-MS intensities of the $[M+H]^+$ and $[M+Na]^+$ ions of (**1**) and (**2**) are useful for characterizing these isomers. The same is true when one wishes to distinguish between (**3**) and (**4**) (Fig. 5). However, these analyses must be conducted under the same experimental conditions; i.e., pH, cone potential and capillary energy, because signal suppression can

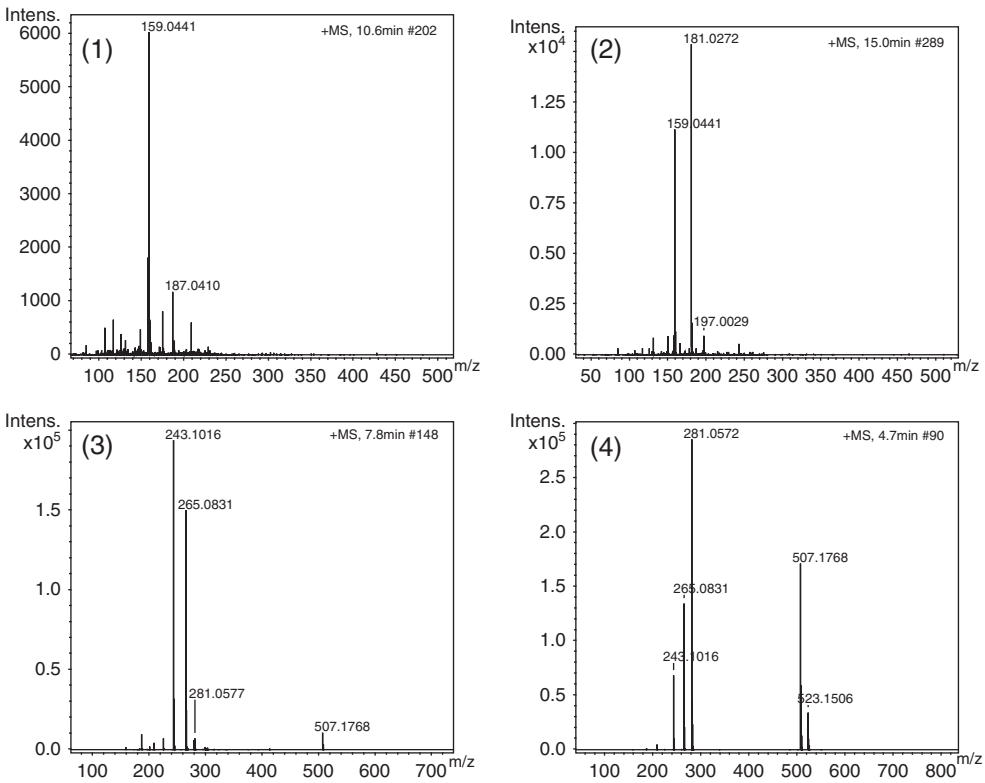

Figure 5. ESI-MS spectra for: (**1**), (**2**), (**3**), and (**4**) in ACN/H_2O (2:1).

Table 1. HR-ESI-MS data (accurate masses and elemental formulae) obtained from the ESI-MS spectra of the quinonoid compounds (**1**)–(**4**) (Fig. 5). Values in parentheses are the errors in ppm for the exact mass

compound	$[M+H]^+$	$[M+Na]^+$	$[M+K]^+$	$[2M+Na]^+$	$[2M+K]^+$
(**1**)	159.0441 $C_{10}H_7O_2^+$ (0)	–	–	–	–
(**2**)	159.0441 $C_{10}H_7O_2^+$ (0)	181.0272 $C_{10}H_6NaO_2^+$ (9.6)	197.0029 $C_{10}H_6KO_2^+$ (15.2)	–	–
(**3**)	243.1016 $C_{15}H_{15}O_3^+$ (0)	265.0830 $C_{15}H_{14}NaO_3^+$ (1.9)	281.0568 $C_{15}H_{14}KO_3^+$ (2.5)	507.1767 $C_{30}H_{28}NaO_6^+$ (2.2)	523.1503 $C_{30}H_{28}KO_6^+$ (2.8)
(**4**)	243.1016 $C_{15}H_{15}O_3^+$ (0)	265.0831 $C_{15}H_{14}NaO_3^+$ (1.6)	281.0572 $C_{15}H_{14}KO_3^+$ (1.09)	507.1768 $C_{30}H_{28}NaO_6^+$ (2.0)	523.1506 $C_{30}H_{28}KO_6^+$ (2.8)

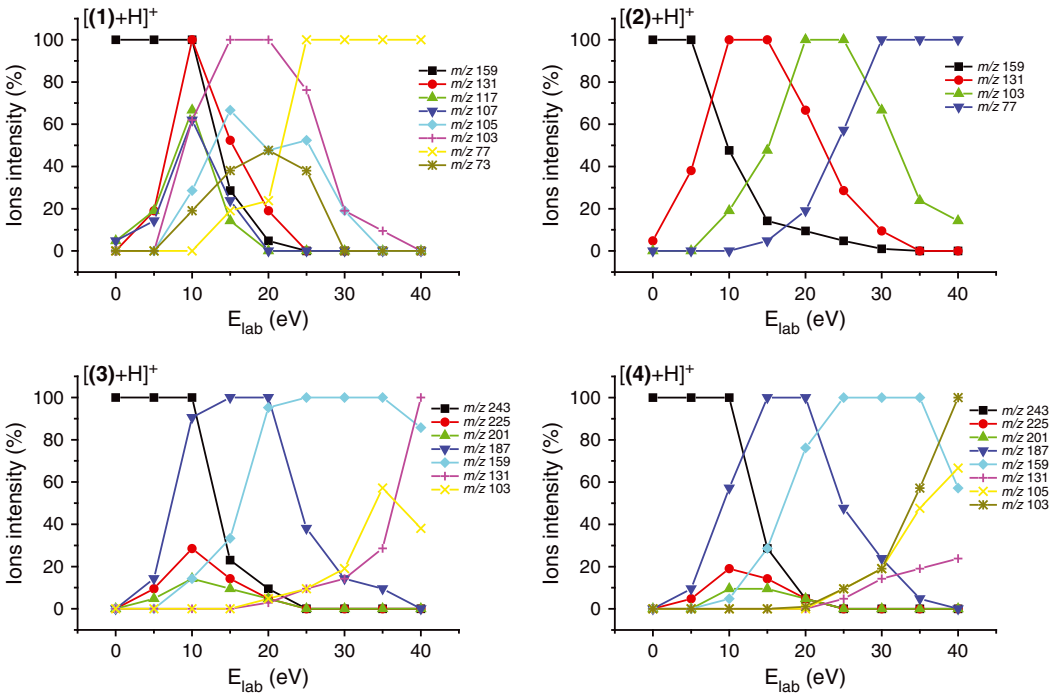

Figure 6. Energy-resolved plots for compounds: $[(\mathbf{1})+H]^+$, $[(\mathbf{2})+H]^+$, $[(\mathbf{3})+H]^+$, and $[(\mathbf{4})+H]^+$. All the MS/MS spectra are available in Supplementary Figs. S2–S5 (see Supporting Information).

occur.[49] Thus, sequential MS is necessary to describe which isomer is being analyzed.[25,26] In this context, ESI-MS/MS analysis can help elucidate the fragmentation mechanism for each compound, and the structure of an unknown compound of this class can be suggested.[25] The major obstacle to the identification of other congeners is that some are isobaric, such as lapachol[24] and isolapachol.[46] Therefore, a more detailed study of the fragmentation of the protonated molecules is mandatory and will be discussed below.

The MS/MS spectra of $[(\mathbf{1})+H]^+$ and $[(\mathbf{2})+H]^+$ present similar product ions (Figs. 6 and 7); some of these ions are diagnostic and help distinguish between (**1**) and (**2**), which is not possible with EI-MS.[29,30]

The ESI-MS/MS spectrum of $[(\mathbf{1})+H]^+$ contains more ions than that of $[(\mathbf{2})+H]^+$. The ions *m/z* 117, and 105 are specific to $[(\mathbf{1})+H]^+$ and can be used to distinguish between 1,4- and 1,2-naphthoquinone. Fragmentation mechanisms for protonated (**1**) and (**2**) were proposed based on the ESI-MS/MS spectra and the energy-resolved plots (Figs. 6 and 7). The dissociation energies were calculated and the Gibbs energies and relative enthalpies of each proposed ion were obtained.

Formation of the *m/z* 131 ion occurs endothermically through ring contraction of $[(\mathbf{1})+H]^+$ or $[(\mathbf{2})+H]^+$ (Schemes 3 and 4). The enthalpies relative to *m/z* 131 were calculated as 11.47 and 16.74 kcal mol^{-1}, respectively. Bayer strain explains the difference in entropy between $[(\mathbf{1})+H]^+$ and the product ion with *m/z* 131 (see relative Gibbs energies and enthalpies values for the *m/z* 131 formation, $\Delta\Delta S = 38$ cal mol^{-1} K^{-1}). The maximum energy transferred by collision (E_{CM})[34] to an ion with *m/z* 159 is approximately 17 kcal mol^{-1} at an E_{lab} of 5 eV. These values are close to those calculated for the enthalpies in this process (Scheme 4).

Formation of the ions at *m/z* 103 and 105 will depend on 1,3-hydrogen migration (Schemes 3 and 4), following collisional activation of *m/z* 159. The critical energy for this migration is 74.6 kcal mol^{-1} (Scheme 3), which should be supplied

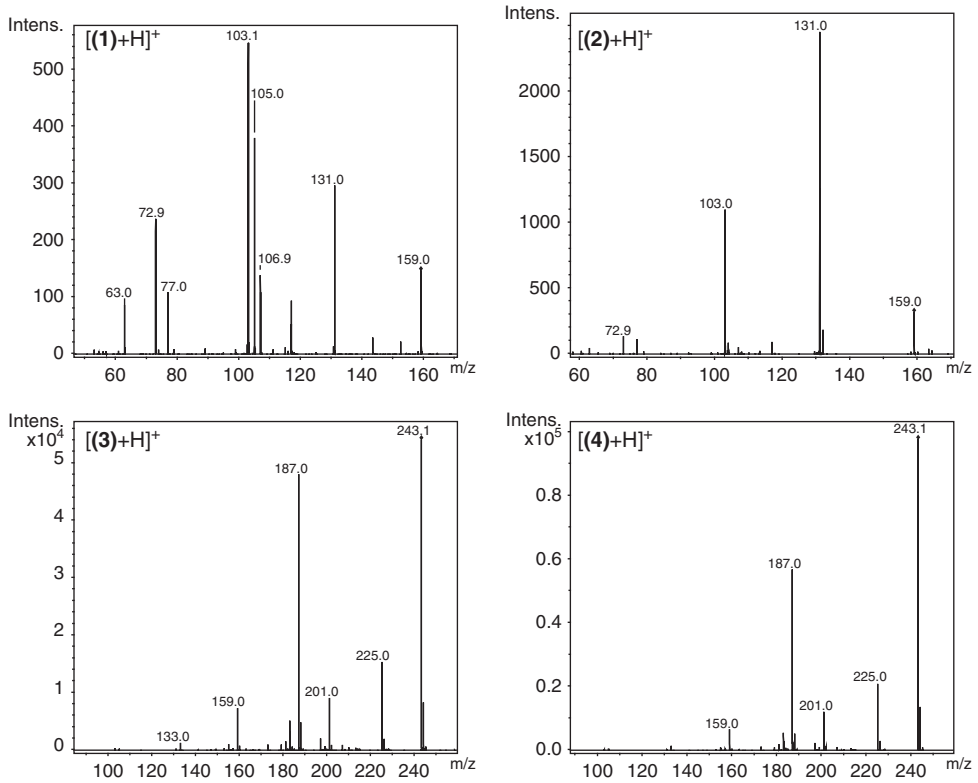

Figure 7. ESI-MS/MS spectra of $[(\mathbf{1})+H]^+$ and $[(\mathbf{2})+H]^+$ at $E_{lab} = 15$ eV (N_2) and $[(\mathbf{3})+H]^+$ and $[(\mathbf{4})+H]^+$ at $E_{lab} = 10$ eV (N_2) (all the spectra are in low resolution).

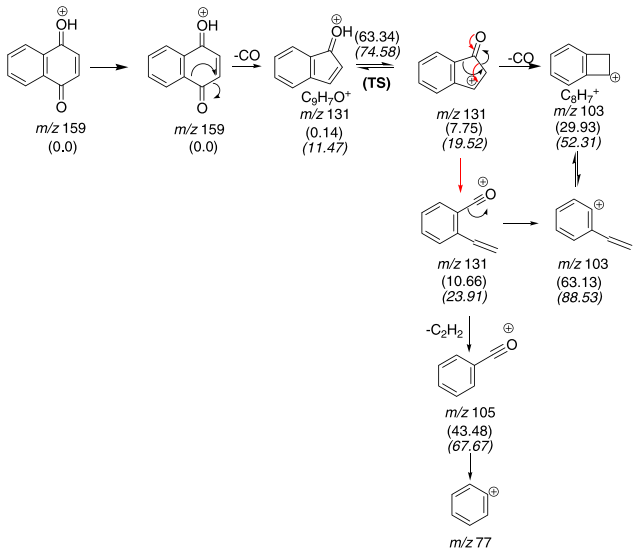

Scheme 3. Fragmentation mechanisms for $[(\mathbf{1})+H]^+$. Values in parentheses are the relative Gibbs energies at 298 K. Italic values are the relative enthalpies at 298 K. Values above arrows are the critical energies of the transition states (TS). All the values are in kcal mol^{-1}, obtained using the B3LYP/6-31+G(d,p) model.

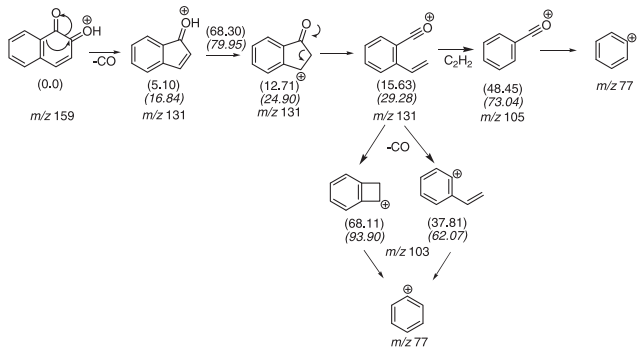

Scheme 4. Fragmentation mechanisms for $[(\mathbf{2})+H]^+$. Values in parentheses are the relative Gibbs energies at 298 K. Italic values are the relative enthalpies at 298 K. Values above arrows are the critical energies of the transition states (TS). All the values are in kcal mol^{-1}, obtained using the B3LYP/6-31+G(d,p) model.

by an E_{lab} of 20 eV, as observed by the increased intensity of the *m/z* 103 ion and decreased intensity of *m/z* 131 ion (Fig. 6). Formation of the *m/z* 103 ion can take place in two distinct ways: (i) CO elimination by a ring contraction, or (ii) acylium ion formation with subsequent CO elimination (Scheme 3).

The ESI-MS/MS spectrum of protonated 1,2-naphthoquinone $[(\mathbf{2})+H]^+$ displays product ions of *m/z* 159, 131, 103, and 77 (Fig. 7). Thus, the absence of the ions at *m/z* 105 and 107 is useful to distinguish protonated 1,2-naphthoquinone $[(\mathbf{2})+H]^+$ from protonated 1,4-naphthoquinone $[(\mathbf{1})+H]^+$.

For $[(\mathbf{2})+H]^+$ dissociation, formation of the *m/z* 131 ion occurs at higher energy than that of the isobaric ion from $[(\mathbf{1})+H]^+$ (Scheme 4). The higher relative enthalpies of the ions generated from $[(\mathbf{2})+H]^+$ confirm this observation, in agreement with the energy-resolved plot of these ions (Fig. 6). Formation of the *m/z* 131 ion from $[(\mathbf{2})+H]^+$ also

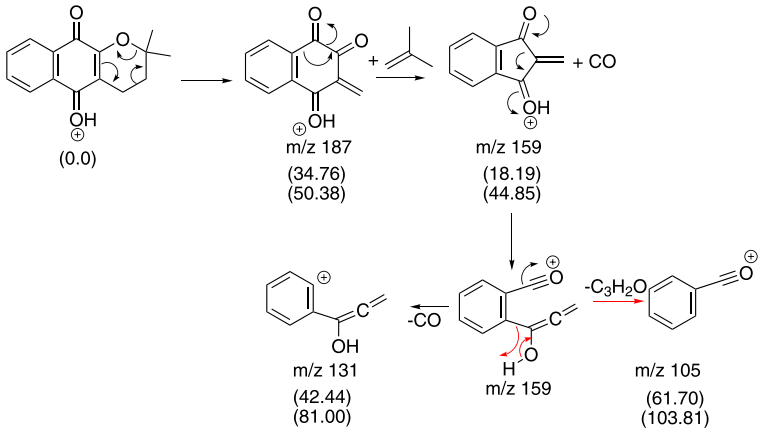

Scheme 5. Fragmentation mechanisms for [(**3**)+H]$^+$. Values in parentheses are the relative Gibbs energies at 298 K. Lower values are the relative enthalpies at 298 K. All the values are in kcal mol^{-1}, obtained using B3LYP/6-31+G(d,p) model.

takes place at a higher value of E_{lab}. The values for the other product ions are also in agreement with the energy-resolved plot.

Using the energy-resolved plots and CID spectra of the similar ions obtained from protonated (**3**) and (**4**) (Figs. 6 and 7), the fragmentation mechanisms shown in Schemes 5 and 6 are proposed for the major ions (*m/z* 187 and 159). Miao *et al.*[20,27] carried out a low-resolution MS/MS analysis of [(**4**)+H]$^+$ and reported results similar those described here, i.e., the most intense ions are *m/z* 187 and 159. These ions are the same as those observed in the analysis of protonated lapachol,[25] which make identification of the precursor protonated molecule confusing. Only the relative intensity of these product ions in the MS/MS spectra of protonated lapachol,[25] α-lapachone, and β-lapachone, recorded under the same conditions, can help distinguish these congeners.

The proposed mechanisms for the formation of the *m/z* 187 ion from [(**3**)+H]$^+$ and [(**4**)+H]$^+$ are very similar to those that occur for the C ring of isoflavones and flavonoids.[50] An RDA reaction[51] occurs with elimination of an alkene and formation of a carbonyl system (Schemes 5 and 6, *m/z* 243 → 187). Early ESI-MS/MS and computational chemistry studies of protonated lapachol and isolapachol showed that this reaction is the major fragmentation process.[24,46] The Gibbs energies of this step are 34.76 and 50.54 kcal mol^{-1} for [(**3**)+H]$^+$ and [(**4**)+H]$^+$, respectively. Analysis of the energy-resolved plot (Fig. 6) and the MS/MS spectra (Fig. 7) shows that formation of the *m/z* 187 ion occurs at a lower energy for [(**3**)+H]$^+$ than for [(**4**)+H]$^+$. An E_{lab} of 10 eV for [(**3**)+H]$^+$ furnishes the *m/z* 187 ion at 100%. For [(**4**)+H]$^+$, this intensity is achieved at an E_{lab} of 15 eV (Figs. 6 and 7). These results agree with those described for the Gibbs energies and enthalpies calculated at the B3LYP/6-31+G(d,p) level.

Thus, the intensity of the *m/z* 187 ion at a known E_{lab} helps differentiate (**3**) and (**4**). Another difference is the intensity of other product ions, such as *m/z* 201 and 159. Formation of the *m/z* 159 ion was attributed to dissociation of the *m/z* 187 ions through CO elimination (*m/z* 187 → 159, Schemes 5 and 6). Formation of *m/z* 159 occurs at lower energy for (**3**) than for (**4**). Analysis of the energy plots and the calculated values for Gibbs energies and relative enthalpies corroborates this attribution. Therefore, the relative enthalpy values (ΔH_{298}) for the formation of *m/z* 159 from (**3**) are lower than from (**4**). The same considerations apply to formation of *m/z* 131 from *m/z* 159. However, two pathways can be suggested for the fragmentation of *m/z* 159: (i) ring contraction and CO elimination, or (ii) cleavage of the five-membered ring with CO elimination and phenylium ion formation (Schemes 5 and 6).

Formation of the *m/z* 225 ion occurs by H_2O loss from *m/z* 243. ESI-MS/MS studies on protonated 2-hydroxy-1, 4-naphthoquinone derivatives showed that water elimination occurs only for molecules with substitution at C(3),[46] due to the stability of the ring opening for H_2O elimination. Studies on lapachol showed that water elimination occurs in the same proportion for α- and β-lapachone. On the other hand, protonation takes place on OH for lapachol, in contrast to the protonation on other 2-hydroxy-1,4-naphthoquinones, where the proton is attached at the O(2) atom. Therefore, the preferred mechanism was H_2O elimination from protonated α- or β-lapachone as depicted for 2-hydroxy-1, 4-naphthoquinone derivatives, using the Grob mechanism, which involves ring opening through acylium formation.[46]

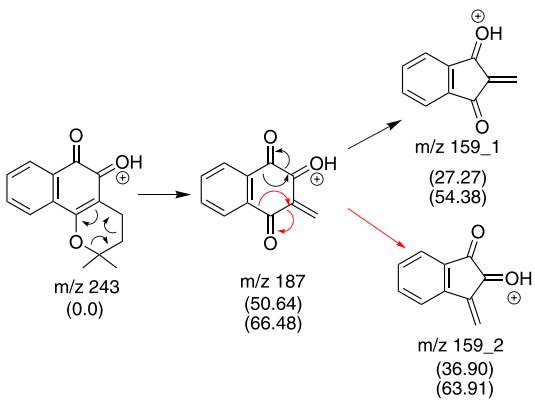

Scheme 6. Fragmentation mechanisms for [(**4**)+H]$^+$. Values in parentheses are the relative Gibbs energies at 298 K. Lower values are the relative enthalpies at 298 K. All the values are in kcal mol^{-1}, obtained using B3LYP/6-31+G(d,p) model.

Rapid Communications in Mass Spectrometry

CONCLUSIONS

ESI-MS studies on 1,2-naphthoquinone and 1,4-naphthoquinone showed that the relative intensities of the protonated and cationized molecules may distinguish between these compounds, without the addition of acid. The same conclusions can be applied to α- and β-lapachone. ESI-MS/MS analyses of protonated 1,2- and 1,4-naphthoquinones have shown that the relative intensity and number of product ions helped characterize these compounds. These results will serve to identify these compounds in complex mixtures or metabolism studies. The fragmentation mechanisms for α- and β-lapachones are very similar. The most intense product ion stems from a RDA reaction, and the different relative intensities of ions during CID experiments distinguish these protonated molecules from their isomers, such as lapachol and isolapachol. Computational results corroborated the ESI-MS and MS/MS data, and all the results can be used in other studies involving naphthoquinones.

SUPPORTING INFORMATION

Supporting information may be found in the online version of this article.

Acknowledgements

The authors thank the Brazilian foundations FAPESP, CAPES, INCT_if and CNPq for financial support. Ricardo Vessecchi thanks FAPESP and CAPES/PNPD for a postdoctoral scholarship.

REFERENCES

[1] S. Patai, Z. Rappaport. *The Chemistry of Quinonoid Compounds*, vol. *II*, John Wiley, New York, **1988**.
[2] T. J. Monks, R. P. Hanzlik, G. M. Cohen, D. Ross, D. G. Graham. Quinone chemistry and toxicity. *Toxicol. Appl. Pharmacol.* **1992**, *112*, 2.
[3] J. H. Lee, J. H. Cheong, Y. M. Park, Y. H. Choi. Down-regulation of cyclooxygenase-2 and telomerase activity by beta-lapachone in human prostate carcinoma cells. *Pharmacolog. Res.* **2005**, *51*, 553.
[4] I. Abraham, R. Joshi, P. Pardasani, R. T. Pardasan. Recent advances in 1,4-benzoquinone chemistry. *J. Braz. Chem. Soc.* **2011**, *22*, 385.
[5] A. V. Pinto, V. F. Ferreira, L. C. M. Coutada. Synthesis of xiloidone and lapachone analogs. *An. Acad. Bras. Ciênc.* **1980**, *52*, 477.
[6] V. F. Ferreira, A. Jorqueira, K. Z. Leal, H. R. X. Pimentel, P. R. Seidl, M. N. Da Silva, M. C. B. V. De Souza, A. V. Pinto, J. L. Wardell, S. M. S. V. Wardell. Preparation of alpha-diazocarbonyl compounds from beta-lapachone derivatives and other 1,2-naphthoquinones: use of the 2D NMR H-1, N-15 and H-1,C-13 HMBC techniques in assigning regiochemistry. *Magn. Reson. Chem.* **2006**, *44*, 481.
[7] D. C. M. Ferreira, I. Tapsoba, S. Arbault, Y. Bouret, M. S. A. Moreira, A. V. Pinto, M. O. F. Goulart, C. Amatore. Ex vivo activities of beta-lapachone and alpha-lapachone on macrophages: a quantitative pharmacological analysis based on amperometric monitoring of oxidative bursts by single cells. *ChemBioChem.* **2009**, *10*, 528.
[8] A. J. Araujo, A. A. de Souza, E. N. Da Silva, J. D. B. Marinho, M. A. B. F. De Moura, D. D. Rocha, M. C. Vasconcellos, C. O. Costa, C. Pessoa, M. O. De Moraes, V. F. Ferreira, F. C. De Abreu, A. V. Pinto, R. C. Montenegro, L. V. Costa-Lotufo, M. O. F. Growth inhibitory effects of 3′-nitro-3-phenylamino nor-beta-lapachone against HL-60: a redox-dependent mechanism. *Toxicol. Vitro* **2012**, *26*, 585.
[9] C. A. Camara, T. M. S. Silva, T. G. Da-Silva, R. M. Martins, T. P. Barbosa, A. C. Pinto, M. D. Vargas. Molluscicidal activity of 2-hydroxy-[1,4]-naphthoquinone and derivatives. *An. Acad. Bras. Ciênc.* **2008**, *80*, 329.
[10] O. Kayser, A. F. Kiderlen, H. Laatsch, S. L. Croft. In vitro leishmanicidal activity of monomeric and dimeric naphthoquinones. *Acta Tropica* **2000**, *77*, 307.
[11] K. Kobayashi, S. Nishiumi, M. Nishida, M. Hirai, T. Azuma, H. Yoshida, Y. Mizushina, M. Yoshida. Effects of quinone derivatives, such as 1,4-naphthoquinone, on DNA polymerase inhibition and anti-inflammatory action. *Med. Chem.* **2011**, *7*, 37.
[12] H. Hussain, K. Krohn, V. U. Ahmad, G. A. Miana, I. R. Green. Lapachol: an overview. *Arkivoc* **2007**, *ii*, 145.
[13] M. N. Da Silva, V. F. Ferreira, M. C. B. V. De Souza. An overview of the chemistry and pharmacology of naphthoquinones with emphasis on beta-lapachone and derivatives. *Quim. Nova* **2003**, *26*, 407.
[14] E. A. Hillard, F. C. De Abreu, D. C. M. Ferreira, G. Jaouen, M. O. F. Goulart, C. Amatore. Electrochemical parameters and techniques in drug development, with an emphasis on quinones and related compounds. *Chem. Commun.* **2008**, *23*, 2612.
[15] J. B. Fenn. Electrospray wings for molecular elephants (Nobel lecture). *Angew. Chem. Int. Ed.* **2003**, *42*, 3871.
[16] M. Karas, R. Kruger. Ion formation in MALDI: the cluster ionization mechanism. *Chem. Rev.* **2003**, *103*, 427.
[17] S. A. McLuckey, J. M. Wells. Mass analysis at the advent of the 21st century. *Chem. Rev.* **2001**, *101*, 571.
[18] P. T. Kasper, M. Rojas-Cherto, R. Mistrik, T. Reijmers, T. Hankemeier, R. J. Vreeken. Fragmentation trees for the structural characterisation of metabolites. *Rapid Commun. Mass Spectrom.* **2012**, *26*, 2275.
[19] A. E. M. Crotti, E. S. Bronze-Uhle, P. G. B. D. Nascimento, P. M. Donate, S. E. Galembeck, R. Vessecchi, N. P. Lopes. Gas-phase fragmentation of gamma-lactone derivatives by electrospray ionization tandem mass spectrometry. *J. Mass Spectrom.* **2009**, *44*, 1733.
[20] X. S. Miao, S. Miao, P. Song, R. E. Savage, C. Zhong, R. Y. Yang, D. Kizer, H. Wu, E. Volckova, M. A. Ashwell, J. G. Supko, X. Y. He, T. C. K. Chan. Identification of the in vitro metabolites of 3,4-dihydro-2,2-dimethyl-2H-naphthol[1,2-b]pyran-5,6-dione (ARQ 501; beta-lapachone) in whole blood. *Drug Metab. Dispos.* **2008**, *36*, 641. X. S. Miao, C. Y. Zhong, Y. X. Wang, R. E. Savage, R. Y. Yang, D. Kizer, E. Volckova, M. A. Ashwell, T. C. K. Chan. In vitro metabolism of beta-lapachone (ARQ 501) in mammalian hepatocytes and cultured human cells. *Rapid Commun. Mass Spectrom.* **2009**, *23*, 12.
[21] R. Vessecchi, P. G. B. D. Nascimento, J. N. C. Lopes, N. P. Lopes. Fragmentation studies of synthetic 2-acylamino-1,4-naphthoquinones by electrospray ionization mass spectrometry. *J. Mass Spectrom.* **2006**, *41*, 1219.
[22] R. Vessecchi, C. A. Carollo, J. N. C. Lopes, A. E. M. Crotti, N. P. Lopes, S. E. Galembeck. Gas-phase dissociation of 1,4-naphthoquinone derivative anions by electrospray ionization tandem mass spectrometry. *J. Mass Spectrom.* **2009**, *44*, 1224.
[23] A. Vasseur, D. Harakat, J. Muzart, J. Le Bras. ESI-MS studies of the dehydrogenative Heck reaction of furans with acrylates using benzoquinone as the reoxidant and DMSO as the solvent. *J. Org. Chem.* **2012**, *77*, 5751.
[24] R. Vessecchi, F. S. Emery, S. E. Galembeck, N. P. Lopes. Fragmentation studies and electrospray ionization mass spectrometry of lapachol: protonated, deprotonated and cationized species. *Rapid Commun. Mass Spectrom.* **2010**, *24*, 2101.

[25] R. Vessecchi, Z. Naal, J. N. C. Lopes, S. E. Galembeck, N. P. Lopes. Generation of Naphthoquinone radical anions by electrospray ionization: solution, gas-phase, and computational chemistry studies. *J. Phys. Chem. A* **2011**, *115*, 5453.
[26] M. L. McKee, M. Balci, H. Kilic, E. Yurtsever. Computational studies of cyclobutadiene and benzocyclobutene fused to p- and o-quinone. *J. Phys. Chem A* **1998**, *102*, 2351; M. M. Balakrishnarajan, R. Hoffmann. Polyhedral boranes with exo multiple bonds: three-dimensional inorganic analogues of quinones. *Angew. Chem. Int. Ed.* **2003**, *42*, 3777.
[27] R. Y. Yang, D. Kizer, H. Wu, E. Volckova, X. S. Miao, S. M. Ali, M. Tandon, R. E. Savage, T. C. K. Chan, M. A. Ashwell. Synthetic methods for the preparation of ARQ 501 (beta-lapachone) human blood metabolites. *Bioorg Med. Chem.* **2008**, *16*, 5635.
[28] M. Niehues, V. P. Barros, F. S. Emery, M. Dias-Baruffi, M. D. Assis, N. P. Lopes. Biomimetic in vitro oxidation of lapachol: a model to predict and analyse the in vivo phase I metabolism of bioactive compounds. *Eur. J. Med. Chem.* **2012**, *54*, 804.
[29] J. H. Bowie, D. W. Cameron, D. H. Williams. Studies in mass pectrometry. I. Mass spectra of substituted naphthoquinones. *J. Am. Chem. Soc.* **1965**, *81*, 5094; D. Becher, C. Djerassi, R. E. Moore, H. Singh, P. J. Scheuer. Mass spectrometry in structural and stereochemical problems. 111. Mass spectrometric fragmentation of substituted naphthoquinones and its application to structural elucidation of echinoderm pigments. *J. Org. Chem.* **1966**, *31*, 3650.
[30] W. G. Stensen, E. Jensen. Structural determination of 1,4-naphthoquinones by mass spectrometry/mass spectrometry. *J. Mass Spectrom.* **1995**, *30*, 1126. V. Krishna, J. Lamba, P. Singh. Conversion of lapachol to array of furano and pyranonaphthoquinone congeners. *J. Ind. Chem. Soc.* **2004**, *81*, 1039.
[31] R. Vessecchi, S. E. Galembeck, N. P. Lopes, P. G. B. D. Nascimento, A. E. M. Crotti. Application of computational quantum chemistry to chemical processes involved in mass spectrometry. *Quim. Nova* **2008**, *31*, 840.
[32] E. Paternó. Richerce sull acido lapachico. *Gazz. Chem. Ital.* **1882**, *12*, 337.
[33] S. C. Hooker. The constitution of lapachic acid (lapachol) and its derivatives. *J. Chem. Soc.* **1892**, *61*, 611.
[34] T. M. Kertesz, L. H. Hall, D. W. Hill, D. F. Grant. Quantifying collision induced dissociation energy for small molecule characterization and identification. *J. Am. Soc. Mass Spectrom.* **2009**, *20*, 1759.
[35] A. D. Becke. A new mixing of hartree-fock and local density-functional theories. *J. Chem. Phys.* **1993**, *98*, 1372. C. T. Lee, W. T. Yang, R. G. Parr. Development of the Colle-Salvetti correlation-energy formula into a functional of the electron-density. *Phys. Rev. B* **1988**, *37*, 785.
[36] R. Ditchfield, W. J. Hehre, J. A. Pople. Self-consistent molecular-orbital methods .9. Extended gaussian-type basis for molecular-orbital studies of organic molecules. *J. Chem. Phys.* **1971**, *54*, 724.
[37] M. J. Frisch, G. W. Trucks, H. B. Schlegel, G. E. Scuseria, M. A. Robb, J. R. Cheeseman, J. A. Montgomery Jr, T. Vreven, K. N. Kudin, J. C. Burant, J. M. Millam, S. S. Iyengar, J. Tomasi, V. Barone, B. Mennucci, M. Cossi, G. Scalmani, N. Rega, G. A. Petersson, H. Nakatsuji, M. Hada, M. Ehara, K. Toyota, R. Fukuda, J. Hasegawa, M. Ishida, T. Nakajima, Y. Honda, O. Kitao, H. Nakai, M. Klene, X. Li, J. E. Knox, H. P. Hratchian, J. B. Cross, V. Bakken, C. Adamo, J. Jaramillo, R. Gomperts, R. E. Stratmann, O. Yazyev, A. J. Austin, R. Cammi, C. Pomelli, J. W. Ochterski, P. Y. Ayala, K. Morokuma, G. A. Voth, P. Salvador, J. J. Dannenberg, V. G. Zakrzewski, S. Dapprich, A. D. Daniels, M. C. Strain, O. Farkas, D. K. Malick, A. D. Rabuck, K. Raghavachari, J. B. Foresman, J. V. Ortiz, Q. Cui, A. G. Baboul, S. Clifford, J. Cioslowski, B. B. Stefanov, G. Liu, A. Liashenko, P. Piskorz, I. Komaromi, R. L. Martin, D. J. Fox, T. Keith, M. A. Al-Laham, C. Y. Peng, A. Nanayakkara, M. Challacombe, P. M. W. Gill, B. Johnson, W. Chen, M. W. Wong, C. Gonzalez, J. A. Pople. *Gaussian 03, Revision C.02*, Gaussian, Inc., Wallingford, CT, **2004**.
[38] G. Lamoureux, A. L. Perez, M. Araya, C. Agüero. Reactivity and structure of derivatives of 2-hydroxy-1,4-naphthoquinone (lawsone). *J. Phys. Org. Chem.* **2008**, *21*, 1022.
[39] P. J. Gaultier, C. Hauw. Structure de 1'α-naphthoquinone. *Acta Crystallogr.* **1965**, *18*, 179; K. E. Wise, A. K. Grafton, R. A. Wheeler. Trimethyl-p-benzoquinone provides excellent structural, spectroscopic, and thermochemical models for plastoquinone-1 and its radical anion. *J. Phys. Chem A* **1997**, *101*, 1160.
[40] R. Vessecchi, J. N. C. Lopes, N. P. Lopes, S. E. Galembeck. Application of the atoms in molecules theory and computational chemistry in mass spectrometry analysis of 1,4-naphthoquinone derivatives. *J. Phys. Chem. A* **2011**, *115*, 12780.
[41] U. C. Singh, P. A. Kollman. An approach to computing electrostatic charges for molecules. *J. Comp. Chem.* **1984**, *5*, 129.
[42] R. F. W. Bader. Definition of molecular structure: by choice or by appeal to observation? *J. Phys. Chem. A* **2010**, *114*, 7431; R. F. W. Bader. A quantum-theory of molecular-structure and its applications. *Chem. Rev.* **1991**, *91*, 893.
[43] M. Butler, P. A. Mañez, G. M. Cabrera. An experimental and computational study on the dissociation behavior of hydroxypyridine N-oxides in atmospheric pressure ionization mass spectrometry. *J. Mass Spectrom.* **2010**, *45*, 536.
[44] AIM 2000, version 2.0, Copyright 2002. AIM2000 Home Page. Available: http://www.aim2000.de; F. Biegler-König, J. Schönbohm. *J. Comp. Chem.* **2002**, *23*, 1489.
[45] U. Varetto. <MOLEKEL 5.4>; Swiss National Supercomputing Centre, Manno, Switzerland.
[46] R. Vessecchi, F. S. Emery, S. E. Galembeck, N. P. Lopes. Gas-phase reactivity of 2-hydroxy-1,4-naphthoquinones: a computational and mass spectrometry study of lapachol congeners. *J. Mass Spectrom.* **2012**, *47*, 1648.
[47] M. H. Amad, N. B. Cech, G. S. Jackson, C. G. Enke. Importance of gas-phase proton affinities in determining the electrospray ionization response for analytes and solvents. *J. Mass Spectrom.* **2000**, *35*, 784.
[48] U. Koch, P. L. A. Popelier. Characterization of C-H-O hydrogen-bonds on the basis of the charge-density. *J. Phys. Chem.* **1995**, *99*, 9747; W. Nakanishi, S. Hayashi, K. Narahara. Atoms-in-molecules dual parameter analysis of weak to strong interactions: behaviors of electronic energy densities versus laplacian of electron densities at bond critical points. *J. Phys. Chem. A* **2008**, *112*, 13595.
[49] N. P. Lopes, C. B. W. Stark, H. Hong, P. J. Gates, J. Staunton. A study of the effect of pH, solvent system, cone potential and the addition of crown ethers on the formation of the monensin protonated parent ion in electrospray mass spectrometry. *Analyst* **2001**, *126*, 1630.
[50] N. Fabre, I. Rustan, E. de Hoffmann, J. Quetin-Leclercq. Determination of flavone, flavonol, and flavanone aglycones by negative ion liquid chromatography electrospray ion trap mass spectrometry. *J. Am. Soc. Mass Spectrom.* **2001**, *12*, 707.
[51] M. P. Patil, R. B. Sunoj. Density functional theory and atoms-in-molecule study on the role of two-electron stabilizing interactions in retro-Diels-Alder reaction of cycloadducts derived from substituted cyclopentadiene and p-benzoquinone. *Org. Biomol. Chem.* **2006**, *4*, 3923.

